

# Analytical Estimation of Doping in a Microwave based PIII System, Implementing Sheath Models

D. Gupta, *Member, IAENG*, J. Jogi, and P. J. George

**Abstract**— Plasma Immersion Ion Implantation (PIII), a high dose-rate implantation technique, has vast applications in the area of semiconductor electronics, in surface modifications of biomaterials and even in the development of various nano-structures. In this technique, the target is immersed in a plasma source, generated through a microwave plasma generation system and the implantation of ions is done by accelerating the ions with a high negative pulse voltage at the target. The dynamics of the ion transport and the implantation process is different from the CII technique. In this paper, the doping mechanism of individual ions in such a single species collisionless PIII system is studied analytically and the net ion doping concentration has also been computed during the propagation of plasma sheaths by implementing the already developed analytical sheath models.

**Index Terms**— microwave multipolar bucket, Plasma immersion ion implantation, sheaths, current density

## I. INTRODUCTION

PLASMA Immersion Ion Implantation (PIII) emulates Beam line Ion Implantation technique in a number of areas, viz., high throughput, fast and efficient implantation, independent of wafer topology, by circumventing line-of-sight restrictions and target masking problems of conventional Implantation technique [1], [2]. In the field of semiconductor electronics, PIII has been successfully implemented in the fabrication of ultrashallow p+/n junctions, conformal doping of trench sidewall in deep trench-based dynamic RAMs, precise control over gate oxide thickness for memory and logic transistors, formation of Silicon on Insulators (SOI) substrates, poly-silicon thin film transistors (TFTs) for flat-panel displays, thin film growth, fabrication of low dielectric constant materials for ULSI multilevel interconnects [3], [4], etc. The researchers are even exploring PIII technique for surface modifications of biomaterials [5], [6] and for the development of nanoscale structures, like, carbon nanotubes, ZnO nanowires, etc. [7]-[9].

In PIII technique, the target to be implanted is immersed

D. Gupta is with Department of Electronic Science, University College, Kurukshetra University, Kurukshetra, INDIA. (phone: +91-9466046333; fax: +91-1744-238035; e-mail: gupty2kuk@yahoo.co.uk).

J. Jogi is with Dept. of Physics & Electronics, ARSD College, University of Delhi, Delhi, INDIA. (e-mail: jogijyotika@rediffmail.com).

P. J. George is with Kurukshetra Institute of Management and Technology (KITM), Kurukshetra University, Kurukshetra INDIA. (e-mail: pj.pjgeorge2@gmail.com).

in a plasma source, generated through a microwave plasma generation system such as MMB (Microwave Multipolar Bucket) and ECR (Electron Cyclotron Resonance) plasmas [10], and the implantation of ions is done by accelerating the ions with a high negative pulse voltage, applied to the target. As a result of negative potential at the target, electrons near the target surface get repelled and a uniform sheath of positive ions called Ion-Matrix Sheath is established around the target. With the electric field, developed around the sheath, the ions accelerate across the sheath and get implanted into the target. As a result, the density of ions within the sheath decreases and enough ions are exposed to keep the same sheath potential. This further develops toward a dynamic sheath called Child-Law Sheath which expands with pulse time. In this study, an MMB type of microwave plasma generation system is considered for PIII doping because of its higher ion density, lower ion energy, and lower contamination levels. As schematic of such a system [11], [12], the plasma is confined in a chamber by a multipolar magnetic field structure, excited by a 2.45GHz microwave source, vacuum, gas handling systems and a target holder (Fig. 1).

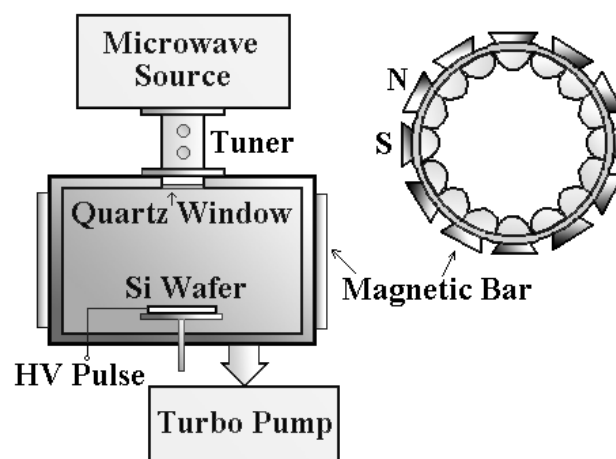


Fig. 1. Microwave multipolar bucket (MMB) plasma system.

The higher ion density and better radial ion density uniformity in the chamber are achieved as electrons are reflected back into the plasma by the magnetic mirror instead of being lost to the chamber walls. The multipolar magnetic structure helps in confinement of plasma as well as in trapping the fast electrons which are further responsible for higher ion density and excellent radial homogeneity of ion density.

In this paper, the sheaths transformation verses pulse time for different type of ions namely Argon, Oxygen, Hydrogen plasmas produced in such a MMB type of system and the effect of different ion masses on sheath propagation and implant doses for one pulse duration in a collisionless PIII system has been analytically studied.

## II. CURRENT DENSITIES AND DOPING CONCENTRATIONS

The assumptions of PIII system for the sheath models are considered as:

- (i) The target with planner geometry.
- (ii) Ideal pulse with no rise and fall times.
- (iii) Only singly charged ions in the plasma.
- (iv) Ion flow is collisionless.

In such a PIII system, the target to be implanted is placed in the microwave generated plasma and short duration pulses with high negative voltage are applied. With the application of a pulse, electrons near the target are reflected back from the target with inverse electron plasma frequency ( $\omega_{pe}^{-1}$ ) and so a uniform sheath of ions called ion-matrix sheath is created having a thickness say  $s_0$ , where  $s_0 = (2\epsilon_0 V_0 / en_0)^{1/2}$ ,  $\epsilon_0$  is free space permittivity,  $e$  is ion charge,  $n_0$  is ion density and  $V_0$  is pulse potential being applied to the target.

The current density ( $j_{IM}$ ) analytically modeled for ion-matrix sheath by Lieberman for such a sheath [13], is :-

$$j_{IM} = \left\{ (en_0 u_0) / \cosh^2(T) \right\} \left\{ \sinh(T) + (2/9) \{ 1 + T \sinh(T) - \cosh(T) \} \right\} \quad (1)$$

where  $u_0 = (2eV_0/M)^{1/2}$  is the ion velocity,  $M$  is the mass of the ion,  $T = \omega_{pi} t_p$ , where  $\omega_{pi} = u_0/s_0$  is ion plasma frequency and  $t_p$  is the pulse time.

As a result, ions in the ion-matrix sheath are drifted into the target, resulting in pushing the sheath-plasma edge further away and uncovering new ions to compensate the ions that have already been implanted. On a longer time scale, the system evolves towards a steady state Child-law sheath.

The current density analytically modeled in general form for Child-law sheath [14] is :-

$$j_{CL} = \frac{2}{9} \frac{eu_0}{\left( \frac{2}{3} \omega_{pi} t K + 1 \right)^{2/3}} \frac{n_k}{\sqrt{c_{k-1}}} \quad (2)$$

where for a single species of plasma in the chamber,  $k=0$ ;  $K=1$ ;  $c_{k-1}=1$ .

For these current densities of Eq. (1) & (2) during the propagation of two types of ion-sheaths, the doping concentration per pulse can be computed by:-

$$d = \frac{1}{e} \int_0^t j_{m,c}(t) dt \quad (3)$$

In this paper, a microwave based plasma generation PIII system is assumed with a plasma density of  $10^{16}$  ions/m<sup>3</sup>. The target is supported by a holder and one plane surface is exposed to the ions. The target holder is isolated from the chamber and is connected to a negative pulse source. To study the effect of ion accelerating potential on doping, negative pulses of amplitude 15KV with pulse duration of 0.2 $\mu$ s are applied independently to the sample. In such a system, the current densities for implantation of singly

charged ions of Argon, Oxygen and Hydrogen as a function of time for one pulse duration are computed implementing both sheath models.

## III. RESULTS

The ion current densities for both sheath models implementing Eq. (1) and Eq. (2) are plotted in Fig. 2. It is observed that in the case of ion-matrix sheath model, the peak current density and the occurrence of peak, are ion mass dependent (Table I).

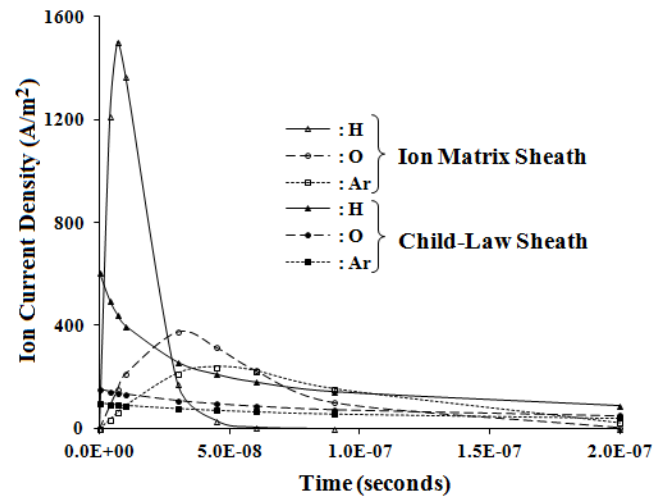


Fig. 2. Ion current density vs. time plot for sheath models at pulse potential of -15KV for 0.2 $\mu$ s duration.

When current densities corresponding to three ions using both the sheath models are plotted simultaneously, the validity of the ion-matrix sheath and the time of propagation of Child-law sheath is estimated. The intersection of current density plots of two models corresponding to each ion is the validity of the existence of ion-matrix sheath and after this time of intersection, the Child-law sheath model decides the current density. This instant of time is decided by the ion mass, which depicts that for the heavier ions the dynamic sheath formation takes place later than that for lighter ions.

In computing the net doping concentrations as a function of time for Ar<sup>+</sup>, O<sup>+</sup> and H<sup>+</sup> ions during both sheaths for one pulse duration of 1.5 $\mu$ s and with 15KV negative pulse potential, Eq. (3) is implemented and is shown in Fig. 3.

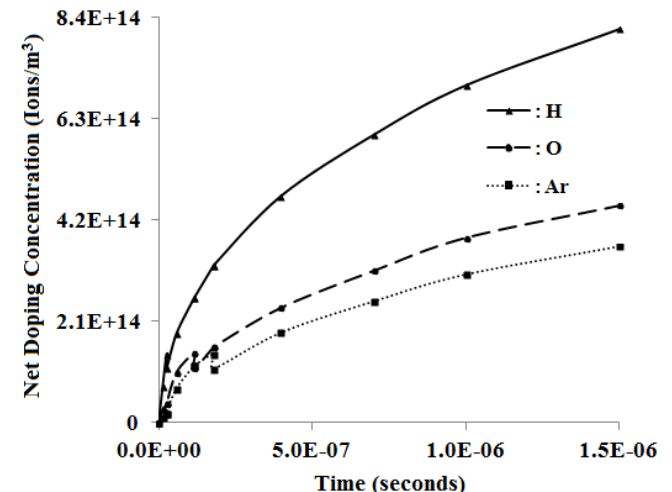


Fig.3. Doping concentration vs. time plot for H, O and Ar ions at pulse potential of -15KV for 1.5 $\mu$ s duration.

It is observed that in the first few nanoseconds of the pulse, for ion-matrix sheath, the doping concentration rises sharply and reaches a maximum value of  $1.42 \times 10^{14}$  at an instant of time corresponding to the point of intersection of the current density plots of the two models. Beyond this point, doping concentration is evaluated only on the basis of Child-law sheath model.

TABLE I

ESTIMATED VALUES OF CREATION TIME, ION CURRENT DENSITY AND DOPING CONCENTRATION FOR DYNAMIC SHEATH AND NET DOPING FOR 1.5 $\mu$ S PULSE DURATION

Ion	Peak current density ( $j_{IM}$ ) A/m <sup>2</sup>	Dynamic sheath creation time (ns)	Dynamic sheath doping	Net doping
Ar	240	180	$4.3 \times 10^{14}$	$5.9 \times 10^{14}$
O	390	115	$5.3 \times 10^{14}$	$6.8 \times 10^{14}$
H	1500	25	$9.3 \times 10^{14}$	$1.1 \times 10^{15}$

At the intersection of the current density plots of the two models, the estimated doping concentration of two models is found to be different. The doping concentration in the case of Child-law sheath model is less than the doping concentration of ion-matrix sheath at that instant of time. However, the doping concentration increases with time beyond this point, and the major contribution to the doping concentration is evaluated using Child-law sheath model. The pulse width decides the desired doping concentration.

#### IV. CONCLUSION

The doping concentration contribution of ion-matrix sheath is valid only in the initial stages of implantation which is followed by the Child-law sheath and the major contribution of doping is due to Child-law sheath model.

The pulse duration requires to be adjusted, to get a desired doping concentration in the target. Therefore, for short duration pulses, both the sheath models are to be considered.

For higher pulse potential, we achieve higher ion current density and hence higher doping concentration.

Higher the ion mass, lesser is the doping concentration in the target for similar type of pulse. Thus, the ion current density and hence the doping concentration are ion dependent.

Thus in a microwave based PIII system, we can theoretically analyze the physics of sheath propagation and the implant doses for different types of singly charged ion species that can further help in predicting the doping profiles in a target.

#### ACKNOWLEDGMENT

Authors gratefully acknowledge the support given by the Kurukshetra University for carrying out this work.

#### REFERENCES

- [1] J. R. Conrad and C. Forest, "Plasma source ion implantation," in *IEEE International Conference on Plasma Science*, Canada, 1986, pp. 28-29.
- [2] C. Jones, B. P. Linder, and N. W. Cheung, "Plasma immersion ion implantation for electronic materials," *Japan Journal of Applied Physics*, vol. 35, pp. 1027-1035, 1996.
- [3] K. Lee, "Plasma immersion ion implantation as an alternative doping tech. for ULSI," in *International Workshop on Junction Technology*, Japan, 2001, pp. 21-27.
- [4] P. K. Chu, "Semiconductor applications of plasma immersion ion implantation," *Plasma Physics and Contr. Fusion*, vol. 45, pp. 555-570, 2003.
- [5] N. Huang, P. Yang, Y. X. Leng, J. Wang, H. Sun, J. Y. Chen, et al., "Surface modification of biomaterials by plasma immersion ion implantation," *Surface and Coatings Technology*, vol. 186, pp. 218-226, 2004.
- [6] P. K. Chu, "Plasma-treated biomaterials," *IEEE Trans. on Plasma Science*, vol. 35, pp. 181-187, 2007.
- [7] Z. J. Han, B. K. Tay, M. Shakerzadeh, and K. Ostrikov, "Superhydrophobic amorphous carbon/carbon nanotube nanocomposites," *Applied Physics Lett.*, vol. 94, pp. 223106-223108, 2009.
- [8] Y. Yang, X. W. Sun, B. K. Tay, H. T. Cao, J. X. Wang, and X. H. Zhang, "Revealing the surface origin of green band emission from ZnO nanostructures by plasma immersion ion implantation induced quenching," *Journal of Applied Physics*, vol. 103, pp. 64307-64310, 2008.
- [9] L. Liao, Z. Zhang, Y. Yang, B. Yan, H. T. Cao, L. L. Chen, et al., "Tunable transport properties of n-type ZnO nanowires by Ti plasma immersion ion implantation," *Journal of Applied Physics*, vol. 104, pp. 76104-76106, 2008.
- [10] S. Qin, N. E. McGruer, C. Chan, and K. Warner, "Plasma immersion ion implantation doping using a microwave multipolar bucket plasma," *IEEE Trans. Electron Dev.*, vol. 39, no. 10, pp. 2354-2358, 1992.
- [11] Z. Zakrzewski and M. Moisan, "Plasma sources using long linear microwave field applicators - main features, classification and modelling," *Plasma Sources Sci. Tech.*, vol. 4, pp. 379-397, 1995.
- [12] L. Pomathiod, R. Debie, Y. Arnal, and J. Pelletier, "Microwave excitation of large volumes of plasma at electron cyclotron resonance in multipolar confinement," *Physics Lett. A*, vol. 106, pp. 301-304, 1984.
- [13] M. A. Lieberman, "Model of plasma immersion ion implantation," *Journal of Applied Physics*, vol. 66, no. 7, pp. 2926-2929, 1989.
- [14] D. Gupta, B. Prasad, J. Jogi, and P. J. George, "A generalized analytical model of a multispecies plasma immersion ion implantation process in a collisionless system," *Journal of Mater. Sci. & Engg. B (ISSN 2161-6221)*, vol. 1, no. 3, 372-377, 2011.